Synthesis and Tribological Performance of Novel MoxW1−xS2 (0 ≤ x ≤ 1) Inorganic Fullerenes

Article *in* Tribology Letters · January 2009

DOI: 10.1007/s11249-009-9493-8

CITATIONS
50

READS
151

4 authors, including:

Fabrice Dassenoy
Ecole Centrale de Lyon
79 PUBLICATIONS **2,783** CITATIONS
SEE PROFILE

Andrew Bruhács
Institut National de la Recherche Scientifique
12 PUBLICATIONS **502** CITATIONS
SEE PROFILE

Wolfgang Tremel
Johannes Gutenberg-Universität Mainz
670 PUBLICATIONS **14,184** CITATIONS
SEE PROFILE

Tribol Lett (2010) 37:83–92
DOI 10.1007/s11249-009-9493-8

ORIGINAL PAPER

Synthesis and Tribological Performance of Novel $Mo_xW_{1-x}S_2$ ($0 \leq x \leq 1$) Inorganic Fullerenes

Johny Tannous · Fabrice Dassenoy · Andrew Bruhács · Wolfgang Tremel

Received: 28 April 2009 / Accepted: 27 July 2009 / Published online: 27 August 2009

Abstract Inorganic fullerene-like (IF) MoS_2 and WS_2 nanoparticles were found to be good friction modifiers and anti-wear additives when dispersed in a lubricant. Their tribological performance seems to be related to the structure, size, and shape of these nanomaterials. The present study describes the tribological properties of a new inorganic fullerene IF-$Mo_xW_{1-x}S_2$ containing both molybdenum and tungsten disulfide under boundary lubrication. $Mo_xW_{1-x}S_2$ amorphous inorganic fullerene nanostructures were synthesized by means of MOCVD using an induction furnace setup. The average diameters range from 25 to 45 nm. Upon variation of the amounts of precursors and S, various solid solutions of IF-$Mo_xW_{1-x}S_2$ were obtained. In addition, a morphological, chemical, and structural analysis of the samples was performed using high resolution scanning electron microscopy (HRSEM), transmission electron microscopy (TEM), and X-ray powder diffraction (XRD). Friction experiments were carried out with a ball-on-flat contact using an environmental tribometer. The results show interesting friction reducing and wear properties of these nanomaterials. The change in the molecule stoichiometry, which led to a variation of particles size but also to a variation of the crystallinity of the particles, affects the tribological performance.

J. Tannous · F. Dassenoy (✉)
LTDS–ECL Ecully, 36 Avenue Guy de Collongue, Ecully 69134, France
e-mail: fabrice.dassenoy@ec-lyon.fr

J. Tannous
e-mail: johny.tannous@ec-lyon.fr

A. Bruhács · W. Tremel
Institut für Anorganische Chemie und Analytische Chemie, Johannes Gutenberg-Universität, Duesbergweg 10–14, Mainz 55099, Germany

Keywords Solid lubrication friction · Anti-wear additives · Friction modifiers · Boundary lubrification friction

1 Introduction

In recent years, one of the main objectives of our industrial society has been to moderate the amount of pollutants entering the earth's atmosphere. The transport sector is among the top contributors to pollution. Herein, considerable amounts of fuel are sacrificed due to friction and wear, whose reduction is currently achieved by the use of lubrication additives such as molybdenum dithiocarbamate (MoDTC) and zinc dithiophosphate (ZnDTP). However, in spite of their remarkable tribological performance, these additives are producing sulfur and phosphorus gas emissions, harmful both for the environment and the health of people. Furthermore, active sulfur and phosphorus act as poison for catalytic converters. The development of new lubrication additives is consequently a reasonable strategy to pursue. In particular, dispersing nanoparticles in a lubricating base-fluid serves as a new model for an environmentally friendlier solution, which is currently being tested in tribology. Many studies have shown the potential of such particles [1–8]. Some of them conclude higher tribological performance in comparison with traditional additives. Due their small sizes (few tens of nanometers) and morphology (spherical or cylindrical) as well as their composition and their specific lubrication mechanism [8, 9], they are regarded as environmentally friendly and offer a real alternative to classical phosphorus and/or sulfur based lubricants. In this context, advanced nanomaterials like inorganic fullerenes (IF) of transition metal dichalcogenides MX_2 (M = Mo, W,…, X = S, Se) have attracted

much interest, since their discovery by Tenne [4]. For instance, IFs can be used as additives for oils or greases to improve anti-friction and anti-wear properties, resulting in large energy savings, lower equipment maintenance costs, improved productivity, and eventually a decline in unnecessary pollution [4–7]. Particularly IF-WS_2 appears to have excellent tribological properties in comparison to typical metal dichalcogenides. The main advantages of IF nanoparticles lie in their spherical shape, which would allow them to act as microscopic ball bearings in junctions, and their nanometer scale enabling them to easily enter in the contact area, as well as their closed structures resulting in the absence of dangling bonds which increases their chemical inertness [10].

Several phenomena have been proposed by Joly-Pottuz et al. [7–9] to explain the outstanding tribological properties of these nanomaterials: IF-fullerene delamination under severe load, formation of tribofilm made of WS_2 sheets on the surface, superlubricity of the sheets and probably a rolling/sliding effect of the particles. Cizaire [6], in their studies on IF-MoS_2, have also shown an exfoliation of the external sheets of IF-MoS_2 during the friction test. Sheets of MoS_2 are liberated directly in the contact area. Schwarz et al. [11] have theoretically confirmed the possibility of delaminating of IF-WS_2. They showed that van der Waals interactions cause strong adhesion to the substrate, which favors the release of delaminated layers onto the surface. As we can see, most studies were carried out on the tribological performance of either IF-WS_2 or IF-MoS_2 nanoparticles, but so far no study was done on the tribological properties of IF-$Mo_xW_{1-x}S_2$ containing both molybdenum and tungsten disulfide. Nath [12] was able to prepare $Mo_{1-x}W_xS_2$ nanotubes by the decomposition of thiometallate solid solutions of the formula $(NH_4)_2Mo_{1-x}W_xS_4$. Such $Mo_{1-x}W_xS_2$ nanotubes would be expected to have different tribological and other properties compared to MoS_2 and WS_2.

In this article, the synthesis of new fullerenes of IF-$Mo_xW_{1-x}S_2$ ($0 \leq x \leq 1$) is reported. Morphological, chemical, and structural analyses of the fullerenes were made with TEM, EDX, and XRD techniques. Tribological properties of these novel nanomaterials used as additives to lubricant were also investigated. Tests were performed in the boundary lubrication regime. The influence of stoichiometry and the structure as well as the nanoparticle size on the tribological properties of the fullerenes are highlighted.

2 Synthesis

The MOCVD synthesis of the IF particles was carried out in a customized reactor described by Tremel et al. [13, 14]. For each reaction, a mixture of various compositions of $Mo(CO)_6$ and $W(CO)_6$ (ABCR 98% and Acros Organics 99%, respectively) was prepared under inert atmosphere and placed into the quartz reactor setup along with the H_2S gas (GHC Gerling, Holz & Co. 99.5% 2.5) under argon reverse flow. Table 1 summarizes all relevant parameters. The central receptor, pointed out in Fig. 1, is heated inductively; hence, the set point of 650 °C is achieved within 20 min with initial heating rates of 100 °C min^{-1}. Prior to all MOCVD reactions, the apparatus was flushed with argon for 30–60 min at 500 mL min^{-1} flow rate. Upon commencing the heating procedure, the flow rate was reduced to 200 mL min^{-1}. The H_2S gas flow was monitored separately using a bubble counter (5 bubbles/s) and the exhaust was bubbled through sodium hydroxide solution to moderate the release of noxious gases into the atmosphere. Once the reactant mixtures mingle and cause turbulences in the top part of the reactor they travel downwards into the hotter zone passing through the vents where the induction receptor is situated. In a typical MOCVD reaction the temperature is maintained for 90–120 min, depending on the amounts of precursor material. The cooling sequence was initiated by simply switching off all heating units and leaving the argon flow at 200 mL min^{-1}. Product was acquired from the inner deposition quartz cylinder under normal atmosphere.

The induction furnace Hüttinger TIG 5/300 is equipped with a EUROTHERM^{TM} 2704 programmable temperature regulator. Krohne flow meters ensure customization possibilities and reproducibility of reaction conditions.

3 Characterization

Prior to performing tribological studies, the samples presented in Table 1 underwent HRTEM, XRD, and EDX analysis as well as EPR investigations. All samples were handled under ambient temperature and ambient atmosphere.

High resolution TEM images were taken with a CCD camera (14-bit GATAN 794MSC) and acquired by Gatan Digital Micrograph software. High-resolution scanning electron microscopy (HRSEM) was carried out on a Zeiss^{TM} Gemini 1530. Samples were prepared on a resin-coated conductive carbon film by pressing the powdered sample onto it and removing the excess.

EPR measurements were carried out on a Bruker Elexsys 580 cw/pulse EPR spectrometer (X-band, ~9.7 GHz mw frequency).

The X-ray powder diffraction Bruker AXS D8 Discover powder diffractometer is equipped with a 2D HiStar detector using CuKα radiation and a graphite monochromator. The GADDS software package [15] was used for data processing. Samples for micro-XRD were measured

Table 1 IF-$Mo_xW_{1-x}S_2$ samples prepared by means of MOCVD which underwent tribological studies

Sample name	x (Mo)	$1 - x$ (W)	m($Mo(CO)_6$) (mg)	m($W(CO)_6$) (mg)	Temperature (°C)
IF-WS_2	0.0	1.0	0	1.800	650
IF-$Mo_{0.2}W_{0.8}S_2$	0.2	0.8	251	1.339	650
IF-$Mo_{0.5}W_{0.5}S_2$	0.5	0.5	660	879	650
IF-$Mo_{0.8}W_{0.2}S_2$	0.8	0.2	1.230	410	650
IF-MoS_2	1.0	0.0	2.040	0	650

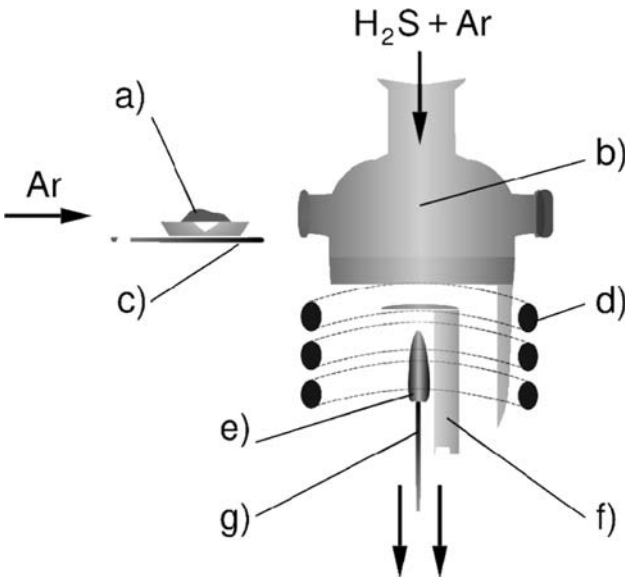

Fig. 1 Standard MOCVD setup. (a) Organometallic precursors ($Mo(CO)_6$ and/or $W(CO)_6$) placed in a ceramic boat, (b) turbulence zone of reactor, (c) thermoelement measuring device wrapped in heating tape, (d) oscillator coils of induction furnace, (e) molybdenum receptor of induction furnace, (f) inner cylinder with vents on bottom, and (g) thermoelement measuring device for receptor. The *arrows* indicate the flow of argon in the apparatus

on a conventional glass microscope slide onto which the sample was fixed with clynol in standard atmosphere.

Transmission electron microscopy (TEM) was performed on FEI–Tecnai. F20 and F30 S-TWIN microscopes with 200 and 300 kV acceleration voltage, respectively and equipped with a FEG electron source, STEM unit and an Oxford EDX spectrometer. Samples for TEM and EDX were prepared by sonicating an ethanolic suspension of the sample for 5–10 s, then depositing 3–5 drops onto a (Plano^{TM}) copper TEM grid with continuous carbon coating.

The morphology determined in HRTEM studies, represented in Figs. 2 and 3 are of spherical IF-type with concentric nested layers showing considerable amounts of point defects and grain boundaries, hereby proving their poorly crystalline character. Nevertheless, the interlayer distance along the c crystal axis was found to be close to the expected 6.3 Å within the crystalline domains. Apart from the $Mo_{0.5}W_{0.5}S_2$ composition in Fig. 3, expected layer bending as seen in the pure phases (Fig. 2) is observed. Synthesis of $Mo_{0.5}W_{0.5}S_2$ yields particles which resemble IFs, but, when viewed in detail, these consist of straight fan-like lamellae as seen in Fig. 3a, b where little layer bending can be witnessed. The pure IF-MoS_2 phase in Fig. 2b exhibits excessive amorphicity in some particles. In general, the particles are agglomerated, possibly a result of dangling bond saturation in incipient stages of growth. Only pure IF-WS_2 shows less agglomeration but rather larger mean particle sizes.

A study of the particle size distributions obtained from TEM footage reveals that the mean diameter of IF-WS_2 is 45 nm while the mixed IFs and also pure IF-MoS_2 vary between 25 and 30 nm, as demonstrated in Fig. 4a–e.

The relative level of point defects was determined indirectly via an EPR study at 20 K which is summarized in Fig. 5, underlining that the $Mo_{0.8}W_{0.2}S_2$ sample contains the largest relative number of dangling bonds. This occurs when, i.e., an S-atom position is vacant in the crystal lattice. The complexity and thus broadening of the signal is an indication for spin-orbit coupling of the unpaired electron with the $I = 5/2$ nuclear spin of Mo. Hence, it is likely that the unpaired electron is within the vicinity of Mo. These point defects and grain boundaries are likely to facilitate exfoliation under friction and shear stress as they structurally destabilize the IF particles. In contrast, pure MoS_2 contains fewer defects. This is likely due to the facile bending of the unperturbed MoS_2 layers.

The wide XRD reflections in Fig. 6 are the result of small crystallite sizes which were witnessed already from the TEM study. Bragg intensities coincide with both 2H and 3R polytypes, whereby the presence of 3R can be mostly deduced from the excessive broadening of the (103) reflection which in turn is equivalent to the (104) and (015) reflections in the 3R polytype. On approaching the pure MoS_2 phase, the crystallinity decreases, mostly visible from the (110), as well as the (112) and (113) reflections for the 2H and 3R polytypes, respectively. The comparable low intensities of the $(002)_{2H}$ and $(003)_{3R}$ reflections are due to texture effects as a consequence of the spherical shape of the IF particles.

The ratio of Mo to W can be verified by performing EDX bulk, point and particle profile scans. The results

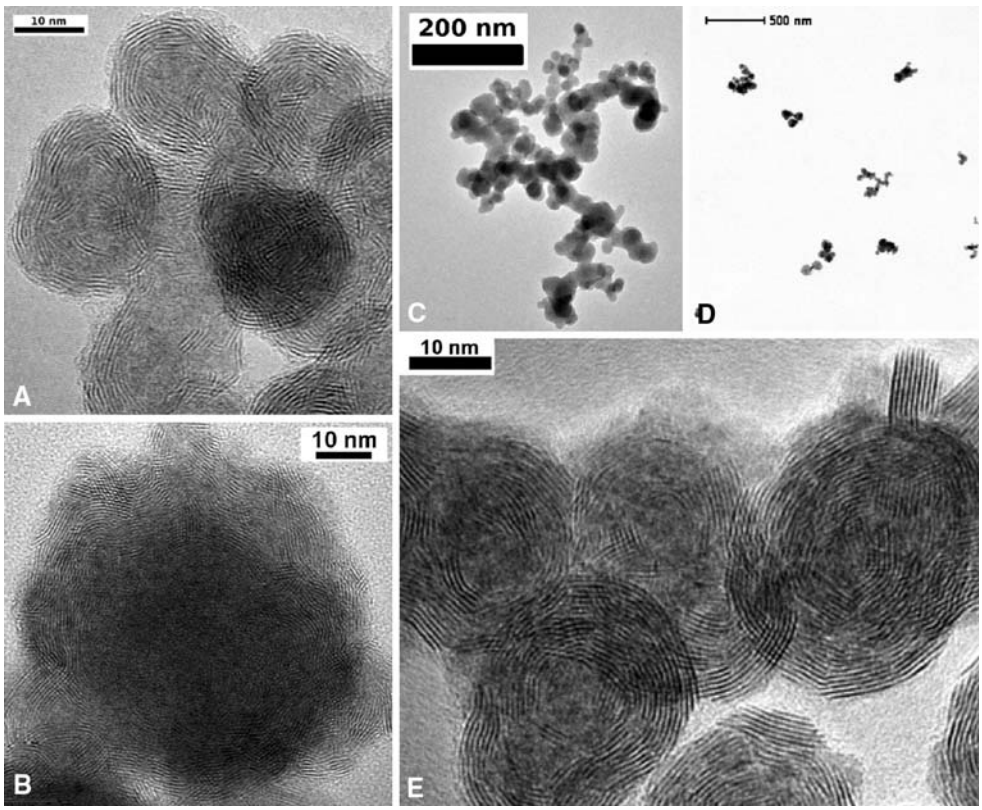

Fig. 2 HRTEM images of pure IF-MoS_2: **a**, **b** and **c**; HRTEM and STEM of IF-WS_2: **d** and **e**, respectively. Subfigure **d** shows reduced agglomeration of WS_2 particles compared to typical MoS_2 agglomerates depicted in **c**. Subfigure **b** demonstrates that some particles can be exceedingly discontinuous in their layers

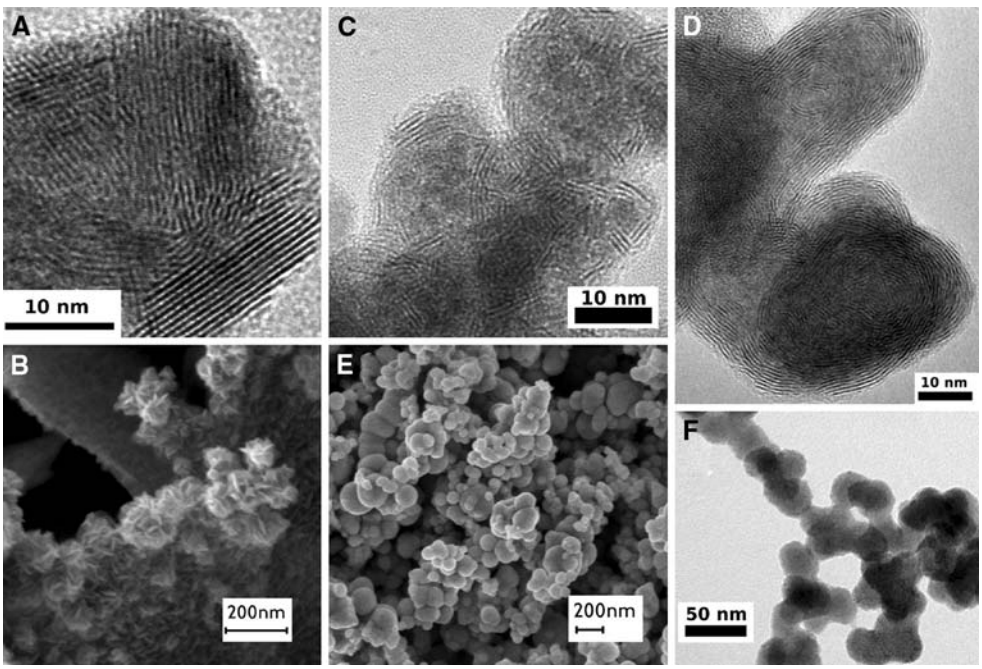

Fig. 3 HRTEM and SEM images. IF-$Mo_{0.5}W_{0.5}S_2$: **a** and **b**. IF-$Mo_{0.8}W_{0.2}S_2$: **c** and **e**, IF-$Mo_{0.2}W_{0.8}S_2$: **d** and **f**. Particles in subfigures **a** and **b** exhibit more exposed lamellae edges and minimal curvature of layers, whereas the latter compositions consist of well behaved nested IF-type structures with bent layers

presented in Figs. 7 and 8 show that both transition elements are present within the IF particles, either as an intra or interlayer solid solution. This is yet to be determined precisely. The analysis reveals only tendencies, as it is not possible to adequately distinguish the molybdenum L-line from the sulfur K-line in EDX since the electronic

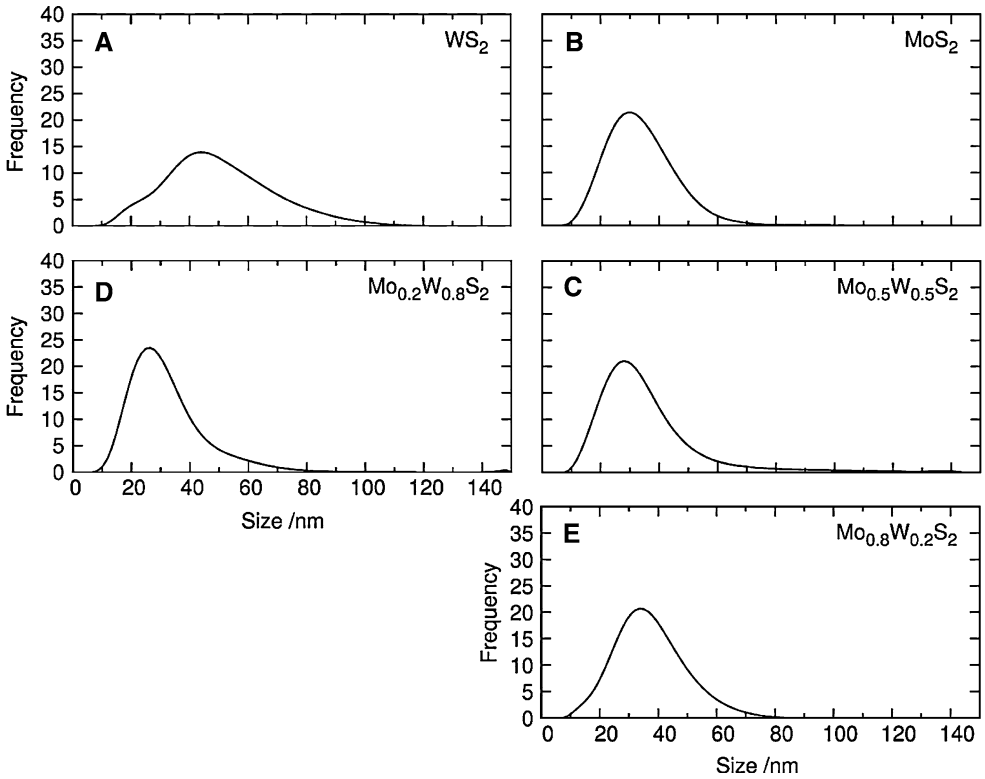

Fig. 4 Particle size distributions derived from TEM image processing for various $Mo_xW_{1-x}S_2$

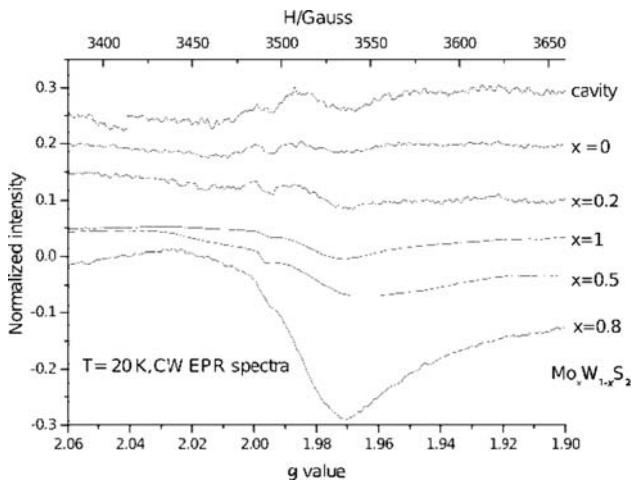

Fig. 5 EPR spectra recorded at 20 K. Pure WS_2 along with $Mo_{0.2}W_{0.8}S_2$ have little defects, whereas samples with Mo $\geq$ 0.5 contain more defects. The broad signal at 1.97 g is attributed to coupling of the nuclear spin I = 5/2 of Mo and the unpaired electrons. "Cavity" refers a measurement without sample contained in the holder

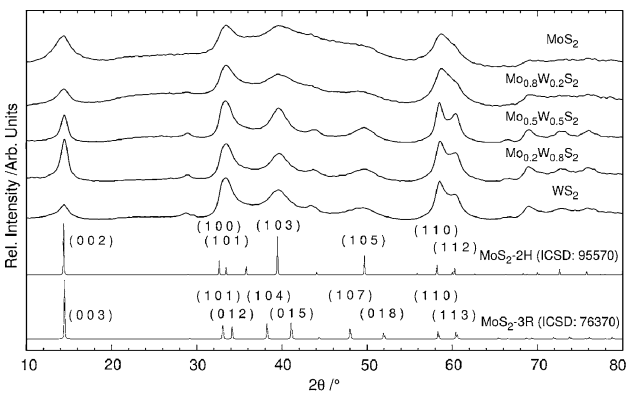

Fig. 6 *Above*: X-ray diffraction powder patterns, *below*: computed XRD patterns based on ICSD data of the hexagonal and rhombohedral MS_2 phases. Pure MoS_2 and $Mo_{0.8}W_{0.2}S_2$ exhibit wider reflections indicating smaller crystallite sizes. Their (110) and (112) as well as (113) reflections are also less defined in comparison to other solid solutions. Both phases 2H and 3R are likely to be present in all particles

transitions are similar in energy. Hence, Mo was quantified using the K-line. Mo is mostly concentrated in the core of the particles while W is more prevalent in the outer shell. This can be attributed to the lower diffusion rate of the $W(CO)_6$ precursor prior to reaction. Mo on the other hand, coalesces faster in the gas phase due to its lower molecular mass and therefore predominates in the core of the particles. However, this is only a tendency that does not significantly undermine the good miscibility of the two transition metals in the 2H- and 3R-MS_2 lattices.

4 Tribological Results

Inorganic fullerenes IF-$Mo_xW_{1-x}S_2$ were tested in a lubricated condition using a pin-on-flat tribometer [16], materials made of polished AISI 52100 steel (Ra = 25 nm). A poly-alphaolefin (PAO 6) oil was used in the present experiments.

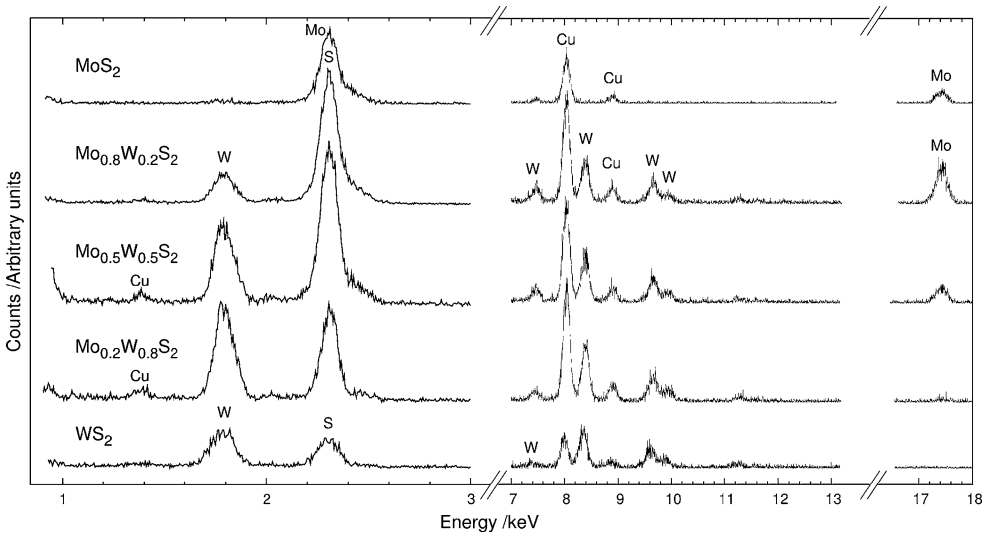

Fig. 7 EDX spectra of studied $Mo_xW_{1-x}S_2$ compositions compared to the respective pure phases (*top* and *bottom*) using overall scans of IF particle agglomerates. The presence of Mo is confirmed by its K transition visible at 17.4 keV. Characteristic W-lines (M transition) are also observed at 1.8 keV. The Cu peak arises due to the usage of copper TEM grids

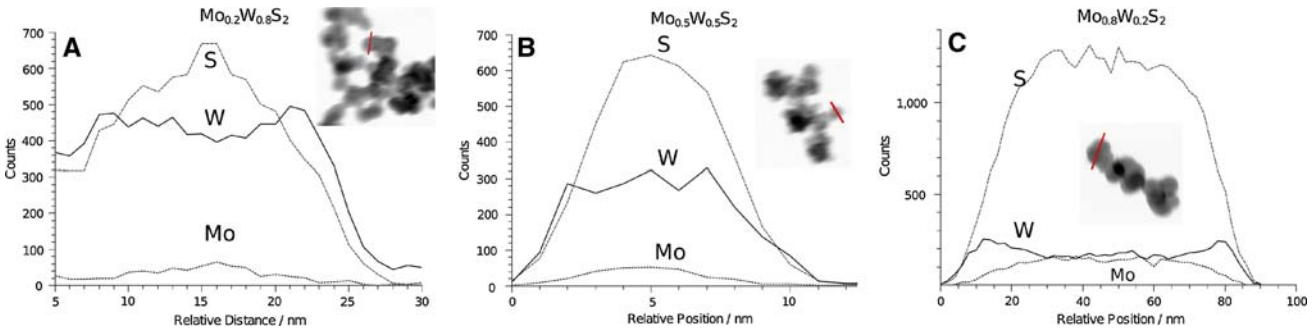

Fig. 8 EDX line scans confirming the presence of both Mo and W within individual particles. Subfigure **a**: $Mo_{0.2}W_{0.8}S_2$, **b**: $Mo_{0.5}W_{05}S_2$ and **c**: $Mo_{0.8}W_{0.2}S_2$. Mo is generally more prevalent in the core of the IFs

Fullerenes were dispersed using an ultrasonic bath at 1 wt% in the PAO. Tribological tests were carried out in ambient air and ambient temperature, with sliding velocity of 2.5 mms^{-1}, and contact pressure of 1.12 and 1.42 GPa (corresponding to normal loads of 5 and 10 N). With these conditions, experiments were performed under boundary lubrication. Figure 9a shows the evolution of the friction coefficient with the number of cycles for the different stoichiometries (and for a contact pressure of 1.12 GPa). Primarily, it can be observed that all stoichiometric variations of IF-$Mo_xW_{1-x}S_2$ considerably reduce friction and therefore the wear of the target surface (Fig. 10) compared to the base oil PAO. However, IF-MoS_2 and $Mo_{0.8}W_{0.2}S_2$ seem to be more effective in reducing friction and wear than the other fullerenes at the same load. For these two compositions, the friction coefficient is below and close to 0.03, respectively. With respect to particles of IF-MoS_2 and IF-WS_2 studied in the literature [6, 7], such a low level of friction has never been previously achieved. At higher contact pressure (1.42 GPa), the difference in friction behavior remains significant between IF-MoS_2 and IF-WS_2 (Fig. 9b). The same tendency as previously was observed for all other compositions (not shown in this figure). $Mo_{0.8}W_{0.2}S_2$ yields a friction coefficient very close but a little bit higher than that obtained with IF-MoS_2. When the stoichiometric variation approaches $x \leq 0.5$, the friction coefficient increases and is similar to that obtained with IF-WS_2.

Optical microscopy observations of the ball wear scars are presented in Fig. 10. The wear scar diameters measured for all the compositions are listed in Table 2 and compared with the calculated Hertz diameter. Regardless of the composition, IFs significantly decrease the wear compared to the pure base oil. However, it can be noted that from $x = 0.5$, the higher the Mo content, the lower the wear. For IF-MoS_2, wear scar is even difficult to observe and its diameter is equivalent to the Hertz diameter. From a general point of view, the wear surfaces with $x > 0.5$ are smoother and shallow than other surfaces.

5 Discussion

Regarding the particle size distributions derived from TEM imaging, it can be concluded that the size of pure IF-MoS_2

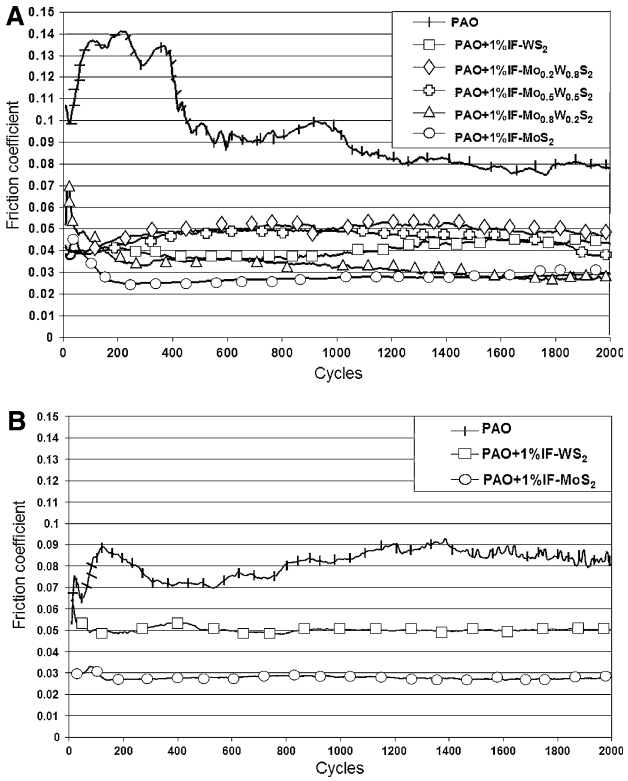

Fig. 9 Evolution of the friction coefficient in a lubricated test for PAO oil and PAO + 1 wt% IF-$Mo_xW_{1-x}S_2$ ($x = 0, 0.2, 0.5, 0.8, 1$) at contact pressure: **a** 1.12 GPa and **b** 1.42 GPa

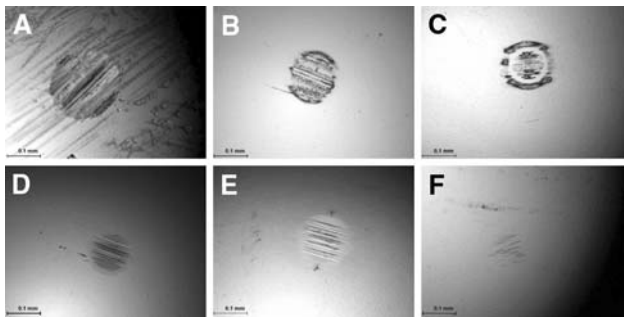

Fig. 10 Pin wear scars at 1.1 GPa: **a** PAO, **b** PAO + 1 wt% IF-WS_2, (**c**) PAO + 1 wt% IF-$Mo_{0.2}W_{0.8}S_2$, **d** PAO + 1 wt% IF-$Mo_{0.5}W_{0.5}S_2$, **e** PAO + 1 wt% IF-$Mo_{0.8}W_{0.2}S_2$, and **f** PAO + 1 wt% IF-MoS_2

nanoparticles and other mixed fullerenes are smaller than those of the IF-WS_2 nanoparticles. This observation could suggest that while exfoliation and third body transfer of molecular sheets onto the asperities is a prevalent mechanism for improved tribological behavior of IF nanoparticles, the size of the particles also plays an important role in improving the tribological properties. Tenne et al. [17] recently synthesized fullerene-like MoS_2 nanoparticles using a new quartz-made reactor. The nanoparticles were found to exhibit high crystalline order with an average size

Table 2 Values of wear scar diameter obtained with PAO and PAO + 1 wt% IF-$Mo_xW_{1-x}S_2$ ($0 \leq x \leq 1$)

Lubricant	Calculated Hertzian wear scar (μm)	Pin wear scar diameter (μm)
PAO	92	206
PAO + 1% IF-WS_2	92	145
PAO + 1% IF-$Mo_{0.2}W_{0.8}S_2$	92	140
PAO + 1% IF-$Mo_{0.5}W_{0.5}S_2$	92	144
PAO + 1% IF-$Mo_{0.8}W_{0.2}S_2$	92	137
PAO + 1% IF-MoS_2	92	94

of 70 nm and comprising more than 30 closed shells. Tribological tests were performed using the same experimental conditions used in the present study. It was found that their well crystallized particles exhibit a friction coefficient as low as 0.03. The size effect was advanced by the authors to explain the difference of friction coefficient obtained between some 120 nm diameter IF-WS_2 particles prepared under similar conditions ($\mu = 0.05$) and the 70 nm diameter IF-MoS_2. It was shown before [7, 10, 18] that large (140 nm) IF-WS_2 nanoparticles could not easily enter the contact area and that their lubricating effect was due to a gradual exfoliation and transfer of molecular sheets onto the asperities of the reciprocating surfaces. The smaller size of the IF-MoS_2 nanoparticles allows them to enter more effectively in between the rubbing surfaces resulting in an improvement of the friction coefficient. Cizaire [6] has studied the tribological properties of IF-MoS_2 nanoparticles prepared by a similar approach (reaction of MoO_3 vapor with H_2S in a reducing atmosphere) but with a different reactor which provided inferior size and shape control. Although very similar in size (60 nm) compared to MoS_2 studied by Tenne et al. [17] the friction coefficient of the lubricant was found to be slightly larger ($\sim$0.055) under similar pressure. Tenne et al. [17] ascribed this difference to the crystalline perfection and the larger number of closed layers of nanoparticles studied in their work. The authors suggest that while exfoliation and third body transfer of molecular sheets onto the asperities is a prevalent mechanism for the improved tribological behavior of the IF nanoparticles, rolling friction could also play a role. Due to the large number of layers which could confer to the nanoparticles higher mechanical resistance, the authors suggest that these fullerenes could be considered to behave as genuine nano-ball bearings precluding gradual deformation and exfoliation giving rise to a very low friction coefficient.

Theoretical studies have described the influence of size and shape of nanoparticles on their tribological properties. Hence, Schwarz [11] have used a scaling approach based on continuum elasticity theory for shells and pairwise summation of van der Waals interactions in order to

investigate theoretically the effect of adhesion, pressure and shear on the deformation, and mechanical stability of spherical nanoparticles. They showed that there are two control parameters which might be used for optimization of the tribological properties in hollow nanoparticles: (1) The ratio between the radius of the particles and the shell thickness which influences the adhesion to the substrate, and (2), the number of defects which contribute to an easier exfoliation of the particles. Thus, for large and thin nanoparticles, van der Waals adhesion can cause considerable deformation and subsequent delamination. Deformation due to VdW interactions are small for thick nanoparticles and the main mechanism for delamination is pressure. In shear flow such thick particles could easily roll in the contact. These results are consistent with the interpretation made by Tenne et al. for their 30 closed shells particles.

Srolovitz [19] highlighted the correlation between the size of the particles, the number of layers, the shape of the particles and the number of defects. Thus, below a critical size depending of the type of particles, stresses/strains induced by the curvature of the layers are so important that the structure must accommodate and introduce dislocations to maintain a spherical/quasi spherical shape. The number of defects would be related to the ratio between the radius of the particles and the number of walls. A small spherical shaped particle can so be described in terms of a relatively large number of low-angle grain boundaries or by a uniform array of dislocations. A small strongly faceted particle indicates the absence of defects. So the dislocations are intrinsic features of onion-type fullerene which serve to relieve the large inherent strains in these structures.

In our study, IF-MoS_2 particles were much smaller (30 nm) than the IF studied in the literature [17, 18]. Their spherical shape is consistent with the fact that they are exceedingly discontinuous in their layers. Their excessive amorphicity can be explained by the synthesis route used to prepare the nanoparticles. The synthesis was carried out without subsequent annealing. Therefore, the degree of their crystallinity is inferior to similar IF nanoparticles synthesized at higher temperatures. As a consequence, the nanoparticles can be made smaller since the bending of the crystalline layers is terminated with occasional defects which allow smaller radius of curvature. The friction coefficient obtained with these particles (0.03) is the same as that obtained by Tenne et al. [17] with well crystallized particles with a diameter of 70 nm (tests performed on the same tribometer with identical experimental conditions). However, in this study, the nano-ball bearing process is difficult to envision. On the other hand, the exfoliation process can be highly enhanced by the large number of defects present in the particles which lead to easier exfoliation of the monomolecular sheets thereafter serving as a third body and providing easy shear between the two metal surfaces. Similar lubricating properties could be obtained with IF nanoparticles of different shape, size and crystallinity, but through two distinct lubrication mechanisms.

Regarding the differences of behavior observed between the different compositions of the mixed IFs presented in this paper friction coefficients are nonetheless very different ranging from 0.05 for $Mo_{0.2}W_{0.8}S_2$ to 0.025 for MoS_2, while the mean particle size remains roughly the same, apart from that of IF-WS_2. This suggests that the size is not the only factor responsible for the different behavior of the various compositions of fullerenes. The stoichiometry and, even more, the different degree of crystallinity between the particles could be one more reason for the change in performance. Thus, if IF-WS_2 are the largest particles, as witnessed from the TEM images, they are also the most crystallized (XRD analysis) and among those which give the highest friction coefficient. In contrast, IF-MoS_2 is among the smallest particles but exhibit also a very poor crystallinity, and their friction coefficient is the smallest. $Mo_{0.8}W_{0.2}S_2$ particles are larger than $Mo_{0.2}W_{0.8}S_2$, but are less crystalline and exhibit an even lower friction coefficient. From a general point of view, it can be deduced from the experiments that the friction coefficient is lower for amorphous particles. Thus, a correlation between the degree of crystallinity of the particles and the friction coefficient appears to be established more easily than a correlation with the particle size. The exfoliation mechanism of the fullerenes could be easier for amorphous particles. The same conclusion is obtained if the reasoning is done from the number of defects-perspective. Regarding EPR measurements and the influence of dangling bonds on the tribological properties of the fullerenes, pure tungsten disulfide IF-WS_2 shows few defects and exhibits the poorest lubrication performance in this test series.

To facilitate the correlation between these key parameters (size, degree of crystallinity, and number of defects) and the lubricating properties of the particles, we reported in Fig. 11 and for different compositions the evolution of

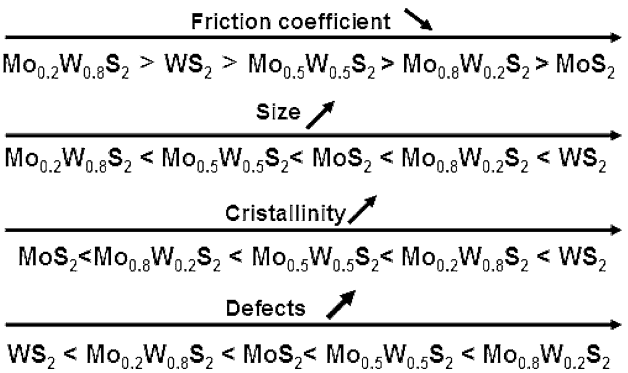

Fig. 11 Evolution of friction coefficient for $Mo_xW_{1-x}S_2$ nanoparticles of different size, crystallinity, and number of defects

the friction coefficient with these parameters. From Fig. 11 one can deduce that the particles are less crystalline, i.e., more amorphous for higher Mo contents, and the more importance can be attributed to the number of defects. Correlation with the size is more precarious. However, the accuracy of this correlation as well as the influence of the tungsten and molybdenum distribution and its indirect consequence on the tribological properties of the particles must be investigated further.

Both, the bulk materials and IF-MoS_2 and IF-WS_2 are known to possess limited durability when used in lubrication that involves a large load and a high rolling/sliding ratio. Previous studies on MoS_2 have concentrated mainly on its use as an extreme pressure additive in lubricating oil and as a lubricant additive in polymeric/metallic composites [17–21]. There has been strong interest in the properties of the MoS_2 composites such as thermal oxidation stability, wear reduction mechanism, rolling contact fatigue and material transfer [22]. This contribution aims to study the tribology and morphology of various solid solutions IF-$Mo_xW_{1-x}S_2$ in frictional experiments. The chemical and tribochemical stability of the different IF-$Mo_xW_{1-x}S_2$ compositions has not been studied in this work.

TEM studies of IF-MoS_2 and IF-$Mo_xW_{1-x}S_2$ and even amorphous MoS_2 (obtained from MOCVD reactions) indicated that these materials are stable under ambient conditions for more than 24 months [23], while previous studies have shown that IF-MoS_2 in moist atmosphere is likely to have a higher oxidation tendency than IF-WS_2 [24]. Bulk WS_2 is thermally more stable and resistant to oxidation (about 50–100 °C) than MoS_2 [25]. The slower oxidation rate of WS_2 can be explained by the formation of tungsten trioxide (WO_3), which is also known to provide a lower friction coefficient than molybdenum trioxide (MoO_3).

Wear is known to induce an oxidation of MoS_2 or WS_2 films, although the integrity of the films is only marginally affected by the tribological runs. XPS measurements indicated massive oxidation of the randomly oriented platelets which are more prone to corrosion than the highly oriented WS_2 films. The oxidation of the films even outside the wear track could be attributed to local overheating of the surroundings during the wear run [24–28].

This oxidation of MoS_2 in air is believed to be dependent not only on temperature, but also on the particle size and availability of air. In particular, particle size plays also an important role in the reactivity of the fullerenes. It has been established that smaller particles have a higher reactivity [22] which may be rationalized by their defect density caused by the radius of curvature. In this context there is only a slight difference between the smaller particles (25 nm) and the largest ones (40 nm). In particular, the average diameter of the composition, which gives the lower friction coefficient (IF-MoS_2) is approximately the same as the composition which displays the highest friction (IF-$Mo_{0.2}W_{0.8}S_2$). The effect of the size on the reactivity of the particles is therefore difficult to judge. However, the distribution of Mo and W in the particles could also have an influence on their tribological properties. It has been shown in this contribution that Mo was predominantly located in the core of the particle whereas W was more localized at the surface. Chemical analysis of the tribofilm is presently under investigation. Preliminary results obtained by XPS analysis show that tribofilms obtained from nanoparticles with a high tungsten content are oxidized more readily (as determined by the presence of WO_3) than the tribofilm obtained from nanoparticles containing less tungsten. It is noteworthy that no oxidation was detected for pristine nanoparticles. The presence of WO_3 could modify the tribological properties of the tribofilm. These results will be reported in a separate contribution.

6 Conclusion

One of the main objectives of this study was to examine the tribological performance of quasi-binary (mixed) IF-$Mo_xW_{1-x}S_2$ nanoparticles obtained by means of an MOCVD setup using H_2S as a chalcogen source. The quasi-binary IF particles exhibit an average diameter of 20–45 nm smaller, i.e., they are significantly smaller than IF nanoparticles studied previously in the literature. Two main conclusions are to be drawn from the results of lubrication and wear tests. (1) All IF samples reduce friction and wear in comparison with the base oil PAO. (2) The best performance was achieved using tungsten doped MoS_2, i.e., $0.5 < x \leq 0.8$ and pure MoS_2. A correlation between the observed EPR signal intensity and number of defects could be deduced. $Mo_{0.8}W_{0.2}S_2$ shows the highest number of defects and exhibits a very poor crystallinity. Its tribological behavior is among the best in the series in terms of friction coefficient and wear reduction. A likely explanation for this finding might be that both, the amorphous character of the particles and the presence of defects, facilitate an exfoliation of layers under external pressure and therefore ameliorate the tribological performance of the material. Moreover, a correlation between the particle size and the friction coefficient could also be made, that is, the larger the diameter of the IF, the poorer is its tribological performance. Nevertheless, the performance of the tested samples surpasses any previously examined IF materials, most likely for the reason that they are very rich in crystal defects, even predominately amorphous. This contributes to the fast exfoliation of the IF nanoparticles. In comparison, pure IF-WS_2 particles appear to have larger diameters. They are better crystallized and had the lowest

number of point defects of all samples. This might be the reason for their relatively poor tribological performance of this material.

Acknowledgments We thank Dr. E. Mugnaioli and Dr. U. Kolb from Mainz Electron Microscopy Centre for TEM analysis. Dr. Ajay Sharma and Dr. Dariush Hinderberger at the Max Planck Institute for Polymer Research, Mainz kindly provided EPR measurements and support in their interpretation. F. Dassenoy thank the Agence Nationale de la Recherche (ANR) for their support.

References

1. Bowden, F.P., Tabor, D.: The Friction and Lubrication of Solids, Part II. Oxford University Press, London (1964)
2. Clauss, F.J.: Solid Lubricants and Self-Lubricating Solids. Academic Press, New York and London (1972)
3. Braithwaite, E.R.: Solid Lubricant and Surfaces, p. 199. Pergamon, Oxford (1964)
4. Tenne, R., Marggulis, L., Genut, M., Hodes, G.: Polyhedral and cylindrical structures of WS_2. Nature **360**, 444–445 (1992)
5. Feldman, Y., Wasserman, E., Srolovitz, D.J., Tenne, R.: Nested inorganic fullerenes and nanotubes. Science **267**, 222–225 (1995)
6. Cizaire, L., Vacher, B., Le Mogne, T., Martin, J.M., Rapoport, L., Margolin, A., Tenne, R.: Mechanisms of ultra-low friction by hollow inorganic fullerene-like MoS_2 nanoparticles. Surf. Coat. Technol. **160**, 282–287 (2002)
7. Joly-Pottuz, L., Dassenoy, F., Belin, M., Vacher, B., Martin, J.M., Fleischer, N.: Ultralow-friction and wear properties of IF-WS_2 under boundary lubrication. Tribol. Lett. **18**, 477–484 (2005)
8. Joly-Pottuz, L., Dassenoy, F., Vacher, B., Martin, J.M.: Ultralow friction and wear behaviour of Ni/Y-based single wall carbon nanotubes (SWNTs). Tribol. Int. **37**, 1013–1018 (2004)
9. Joly-Pottuz, L., Dassenoy, F., Martin, J.M., Belin, M., Montagnac, G., Reynard, B., Fleischer, N.: Pressure-induced exfoliation of inorganic fullerene-like WS_2 particles in a Hertzian contact. J. Appl. Phys. **99**, 23524–23529 (2006)
10. Rapoport, L., Feldman, Y., Homyonfer, M., Cohen, H., Sloan, J., Hutchison, J.L., Tenne, R.: Inorganic fullerene-like material as additives to lubricants: structure–function relationship. Wear **225**, 975–982 (1999)
11. Schwarz, U.S., Komura, S., Safran, S.A.: Deformation and tribology of multi-walled hollow nanoparticles. Europhys. Lett. **50**(6), 762–768 (2000)
12. Nath, M., Mukhopadhyay, K., Rao, C.N.R.: $Mo_{1-x}W_xS_2$ nanotubes and related structures. Chem. Phys. Lett. **352**, 163–168 (2002)
13. Etzkorn, J., Therese, H.A., Rocker, F., Zink, N., Kolb, U., Tremel, W.: Metal-organic chemical vapor deposition synthesis of hollow inorganic-fullerene-type MoS_2 and $MoSe_2$ nanoparticles. Adv. Mater. **17**, 2372–2375 (2005)
14. Zink, N., Pansiot, J., Kieffer, J., Therese, H.A., Panthofer, M., Rocker, F., Kolb, U., Tremel, W.: Selective synthesis of hollow and filled fullerene-like (IF) WS_2 nanoparticles via metal–organic chemical vapor deposition. Chem. Mater. **19**, 6391–6400 (2007)
15. GADDS 4.1.19, Bruker AXS, Madison, Wisconsin, USA (2005)
16. Belin, M.: Triboscopy: a new quantitative tool for microtribology. Wear **168**, 7–12 (1993)
17. Rosentsveig, R., Gorodnev, A., Feuerstein, N., Friedman, H., Zak, A., Fleisher, N., Tannous, J., Dassenoy, F., Tenne, R.: Fullerene-like MoS_2 nanoparticles and their tribological behavior. Tribol. Lett. (in press)
18. Rapoport, L., Bilik, Y., Feldman, Y., Homyonfer, M., Cohen, S.R., Tenne, R.: Hollow nanoparticles of WS_2 as potential solid-state lubricants. Nature **387**, 791–793 (1997)
19. Srolovitz, D.J., Safran, S.A., Homyonfer, M., Tenne, R.: Morphology of nested fullerenes. Phys. Rev. Lett. **74**, 1779–1782 (1995)
20. Mahalu, D., Peisach, M., Wold, A., Tenne, R.: Controlled photocorrosion of WSe_2: influence of molecular oxygen. J. Phys. Chem. **94**, 8012–8013 (1990)
21. Li, X., Gao, Y., Xing, J., Wang, Y., Fang, L.: Wear reduction mechanism of graphite and MoS_2 in epoxy composites. Wear **257**, 279–283 (2004)
22. Matsui, M., Kakishima, H.: Improvement of tribological performance of steel by solid lubricant shot-peening in dry rolling/sliding contact wear tests. Wear **260**, 669–673 (2006)
23. Bruhács, A.: Diploma thesis, Universität Mainz (2008)
24. Schuffenhauer, C., Wildermuth, G., Felsche, J., Tenne, R.: How stable are inorganic fullerene-like particles? Thermal analysis (STA) of inorganic fullerene-like NbS_2, MoS_2, and WS_2 in oxidizing and inert atmosphere in comparison with the bulk material. Phys. Chem. Chem. Phys. **6**, 3991–4002 (2004)
25. Bhushan, B., Gupta, B.K.: Handbook of Tribology. McGraw-Hill, New York (1991)
26. Cohen, S.R., Rapoport, L., Ponomarev, E.A., Cohen, H., Tsirlina, T., Tenne, R., Lévy-Clément, C.: The tribological behavior of type II textured MX_2 (M = Mo, W; X = S, Se) films. Thin Solid Films **324**, 190–197 (1998)
27. Prasad, S.V., McDevitt, N.T., Zabinski, J.S.: Tribology of tungsten disulfide films in humid environments: the role of a tailored metal–matrix composite substrate. Wear **230**, 24–34 (1999)
28. Wong, K.C., Lu, X., Cotter, J., Eadie, D.T., Wong, P.C., Mitchell, K.A.R.: Surface and friction characterization of MoS_2 and WS_2 third body thin films under simulated wheel/rail rolling–sliding contact. Wear **264**, 526–534 (2008)